www.elsevier.com/locate/jbiomech

Sensitivity of predicted muscle forces during gait to anatomical variability in musculotendon geometry

Lode Bosmans, Giordano Valente, Mariska Wesseling, Anke Van Campen, Friedl De Groote, Joris De Schutter, Ilse Jonkers

PII: S0021-9290(15)00144-X
DOI: http://dx.doi.org/10.1016/j.jbiomech.2015.02.052
Reference: BM7068

To appear in: *Journal of Biomechanics*

Accepted date: 28 February 2015

Cite this article as: Lode Bosmans, Giordano Valente, Mariska Wesseling, Anke Van Campen, Friedl De Groote, Joris De Schutter, Ilse Jonkers, Sensitivity of predicted muscle forces during gait to anatomical variability in musculotendon geometry, *Journal of Biomechanics,* http://dx.doi.org/10.1016/j.jbiomech.2015.02.052

Original article

Sensitivity of predicted muscle forces during gait to anatomical variability in musculotendon geometry

[1,*]Lode Bosmans, [2]Giordano Valente, [1]Mariska Wesseling, [3]Anke Van Campen, [3]Friedl De Groote, [3]Joris De Schutter and [1]Ilse Jonkers.

[1]KU Leuven, Department of Kinesiology, Human Movement Biomechanics, Tervuursevest 101, B-3001 Heverlee, Belgium

[2]Laboratorio di Tecnologia Medica, Istituto Ortopedico Rizzoli, via di Barbiano 1/10 , 40136 Bologna, Italy

[3]KU Leuven, Department of Mechanical Engineering, Division PMA, Celestijnenlaan 300B, B-3001 Heverlee, Belgium

*Corresponding author:

Lode Bosmans

Tervuursevest 101, box 1501

3001 Heverlee

Belgium

lode.bosmans@faber.kuleuven.be

Tel: +32 16 329009

Word count: 3421

Abstract

Scaled generic musculoskeletal models are commonly used to drive dynamic simulations of motions. It is however, acknowledged that not accounting for variability in musculoskeletal geometry and musculotendon parameters may confound the simulation results, even when analysing control subjects. This study documents the three-dimensional anatomical variability of musculotendon origins and insertions of 33 lower limb muscles determined based on magnetic resonance imaging in six subjects. This anatomical variability was compared to the musculotendon point location in a generic musculoskeletal model. Furthermore, the sensitivity of muscle forces during gait, calculated using static optimization, to perturbations of the musculotendon point location was analyzed with a generic model. More specific, a probabilistic approach was used: for each analyzed musculotendon point, the three-dimensional location was re-sampled with a uniform Latin hypercube method within the anatomical variability and the static optimization problem was then re-solved for all perturbations. We found that musculotendon point locations in the generic model showed only variable correspondences with the anatomical variability. The anatomical variability of musculotendon point location did affect the calculated muscle forces: muscles most sensitive to perturbations within the anatomical variability are iliacus and psoas. Perturbation of the gluteus medius anterior, iliacus and psoas induces the largest concomitant changes in muscle forces of the unperturbed muscles. Therefore, when creating subject-specific musculoskeletal models, these attachment points should be defined accurately. In addition, the size of the anatomical variability of the musculotendon point location was not related to the sensitivity of the calculated muscle forces.

Keywords: subject-specific musculoskeletal models, sensitivity analysis, anatomical variability, muscle forces, dynamic simulations.

1 Introduction

Instrumented gait analysis is a useful tool to analyze human locomotion. However, it does not allow measurements of individual muscle forces and their contribution to movement coordination in vivo (Zajac et al., 2002; Zajac et al., 2003). Musculoskeletal models (MSM) in combination with multibody-dynamics simulations of movement have therefore been used to study muscle loading and coordination (Erdemir et al., 2007; Fregly, 2009; Pandy and Andriacchi, 2010). Since determining the MSM parameters is still a major challenge, sensitivity analyses have been performed to investigate how the variability of specific model parameters affect the calculated output quantities (e.g., Pal et al., 2007; Lenaerts et al., 2008; Ackland et al., 2012; Dumas et al., 2012; Viceconti et al., 2012; Valente et al., 2013).

Sensitivity analyses are highly relevant for musculoskeletal models given the numerous modeling assumptions on geometric and dynamics parameters. While several studies investigated the sensitivity of calculated muscle forces to perturbations of the muscletendon (MT) force-generating parameters (Scovil and Ronsky, 2006; Xiao and Higginson, 2010; De Groote et al., 2010, Ackland et al., 2012), few studies evaluated the influence of the locations of the points defining the MT-path on the predicted muscle forces during gait. Carbone et al. applied a fixed size perturbation to each MT-point location, which directly affected moment arm length (MAL), and evaluated the isolated effect on muscle forces (Carbone et al., 2012). A recent study perturbed MT-point location, amongst other model parameters, and analyzed the effect on calculated muscle forces and joint contact forces (Valente et al., 2014).

The approach of Carbone has two limitations. Firstly, the induced perturbation (±1cm) does not reflect the anatomical variability of the MT-points. This is particularly relevant in generic MSMs that, to the best of our knowledge, were not evaluated against anatomical variability of MT-points in a control cohort. Secondly, a perturbation-based analysis with single input values prevents investigating the effect of different three dimensional (3D) MT-point location variables according to the established anatomical variability. Such relationship between the anatomical variability of MT-points and the concomitant effect on calculated muscle forces has not been extensively studied. The study of Valente

was based on only one subject-specific model and estimated the size of the MT-point location, but irrespective of anatomical variability.

The aim of the present study was: first, to quantify the anatomical variability of the MT-point locations, and second, to analyze how muscle forces predicted with a scaled-generic MSM are affected by the anatomical variability of the major muscles actuating hip and knee. These questions have been addressed using MRI-based MSM of six control subjects and performing a Monte-Carlo analysis of multibody-dynamics simulations of gait.

Methods

The workflow is presented in figure 1.

Experimental data

Six healthy subjects without orthopaedic problems or previous surgery participated in this study (3 males and 3 females, age: 22.5±2.9yrs, weight: 61.2±1.6kg, height: 172.9±6.9cm). All procedures were approved by the local ethical committee and subjects gave written informed consent.

MRI data of the lower limbs were collected. Five axial images series were acquired on a 3T Siemens MR scanner using a T1 weighted SE sequence with the subjects lying supine with extended knees. With an inter-slice distance of 1 mm, a voxel size of 1.04 x 1.04 x 1 mm obtained for the hip and knee. The voxel size was 1.04 x 1.04 x 2 mm at the femur shaft. A full leg image was created extending from the superior rim of the iliac crest to the distal margin of the toes (Scheys et al., 2006).

For one female subject of this group (23yrs, 63kg, 173cm), gait data were collected during walking at 4 km/h on an instrumented treadmill (Forcelink, Culemborg, The Netherlands). Active infrared markers were placed on 19 anatomical landmarks as well as on six technical clusters (Jansen et al., 2012). 3D marker movement was captured using two Krypton cameras (Nikon Metrology, Leuven, Belgium) at a sampling frequency of 100Hz. Ground reaction forces were measured at a sampling frequency of 1000Hz, using two treadmill-embedded force plates. A representative gait trial was selected.

Musculoskeletal modelling

Using a custom built workflow, six subject-specific MSM were defined based on the MR images, (Scheys et al., 2006). Bone structures (pelvis, bilateral femur and tibia) were defined as volumetric meshes (Mimics, Leuven, Belgium). Body reference frames were defined according to the ISB recommendations (Wu et al., 2002). The paths of all MT-actuators attaching to the pelvis and upper leg (listed in Supplementary materials 2) were defined bilaterally as a line-of-action model running from origin to insertion (Scheys et al., 2006). The number and relative positioning of the MT-point locations defining the MT-paths were set according to the Gait2392 generic model (Delp et al., 2007). The segmentation complexity to accurately segment the muscles spanning the ankle joint guided this selection. MT-point locations of these muscles were adopted from the generic model. This approach is in accordance with Scheys et al. (2006). MT-points were placed so that the muscle line of action was approximated as closely as possible. The insertion points of the quadriceps on the patella were not included in the analysis.

For the one subject that performed the gait analysis, the Gait2392 generic model was scaled based on a static measurement, using a least-squares optimization implemented in OpenSim 3.0.

Anatomical variability of MT-points

The anatomical variability of each of the 91 MT-point locations was determined based on the six MRI-based MSMs. Each MT-point was categorized as origin (o), pseudo origin (po, most distal intermediate point on the proximal segment), pseudo insertion (pi, most proximal intermediate point on the distal segment), insertion (i) or any intermediate via point (via) according to Carbone et al. (2012). For each MRI-based MSM, the location of each MT-point was expressed relative to the bone dimensions. This resulted in 12 relative locations for each individual MT-point. The minimal and maximal relative values defined the anatomical range for that specific MT-point. This range was then transformed to the corresponding segment of the scaled generic model used to generate the dynamic simulations. This transformation was based on fitting anatomical landmarks located on the generic and personalized bone geometry respectively.

Dynamic simulations of gait

Based on the experimental data and the scaled generic model, simulations of one gait cycle were generated in OpenSim 3.0. Joint kinematics were calculated using a Kalman smoothing algorithm (De Groote et al., 2008). A residual reduction algorithm (Thelen et al., 2006) was applied to increase dynamic consistency between kinematics and ground reaction forces. Static optimization was used to calculate muscle forces that produce the joint moments, while minimizing the sum of muscle activations squared. This set of muscle forces is referred to as the nominal dataset.

A Monte-Carlo analysis was then performed defining a subset of the MT-point locations as statistical input variables. Subset selection was based on two conditions: (1) perturbation of the MT-point location influenced the muscles' MAL (cfr. Carbone et al., 2012) and (2) peak nominal MT-force was more than 10% of the maximum isometric force in the reference simulation. Fifty-one MT-points met these two criteria. For each MT-point, the anterior-posterior (AP), superior-inferior (SI) and medio-lateral coordinate in the body reference frame of the scaled generic model were uniformly sampled independently within their specific anatomical variability using a uniform Latin Hypercube Sampling strategy (McKay et al., 1979). This approach ensures full coverage of the range of each variable, by randomly distributing the values of each variable in equiprobable intervals and then randomly permuting the values (Valente et al., 2013, 2014).

The generic model was then updated by generating a perturbed model for each sample of each individual MT-point location, therefore changing the MAL of the perturbed muscle. The optimal fiber length and the tendon slack length were linearly scaled to the new resting length of the MT-actuator (Delp, 2007). Due to the geometrical perturbation, the moment generating capacity of the perturbed muscle are changed. The static optimization problem was then re-solved using each model. This probabilistic approach assessed all possible 3D MT-point location within the anatomical range and analysed the muscle forces. Two hundred simulations per sampled MT-point location ensured that, over the last 10% of the simulations, the change in mean and standard deviation of each perturbed muscle force was less than 2% of its final mean and standard deviation (Valente et al., 2013). This resulted in a total of 10200 simulations run.

Data analysis

The results were post-processed to evaluate the anatomical variability of the MT-points, the local sensitivity (LS) and the overall sensitivity (OS) of calculated muscle forces, described as follows.

Average anatomical ranges along the AP, SI and ML dimension were calculated for all MT-points belonging to the same body segment (i.e., pelvis, femur, tibia). Both absolute variability (cm) and relative variability (% of bone dimension) were reported for the unscaled generic model. The absolute variability allows comparison with fixed perturbation of ±1cm in the study of Carbone et al. (2012). The relative variability allows identifying the MT-points with the largest relative variability.

Two output parameters were modified from Carbone et al. (2012). The LS of the predicted muscle forces, i.e. the effect of perturbation of a MT-point on the corresponding muscle force and moment was evaluated. For each simulation and each muscle, the perturbed muscle force (F_{pert}) at the time instant of maximal muscle force in the nominal simulation (t_{nom}) was identified. This way the change in muscle force is only related to the perturbed MT-point location and not by another kinematic configuration, as the segmental alignment on a different time instant would also affect MAL. Firstly, for each perturbed MT-point, the average and standard deviation of F_{pert} at t_{nom} ($\bar{F}_{pert}$ and LS_{mtp} respectively) over the 200 simulations were calculated at t_{nom}. LS_{mtp} reflects the sensitivity of each muscle force to perturbation of specific MT-points.

Secondly, the difference between $\bar{F}_{pert}$ and the nominal muscle force at t_{nom} (F_{nom}) was calculated:

$$\Delta F = \overline{F}_{pert} - F_{nom}$$

The OS of the muscle force calculation, i.e. the effect of one MT-point perturbation on the force of all unperturbed muscles in the model was evaluated in two ways:

Firstly, for each perturbed MT-point, the average difference in calculated muscle forces of all unperturbed muscles when perturbing a specific MT-point (OS_{mtp}) was calculated as follows:

$$OS_{mtp} = \frac{\sum_{i=1}^{n_{unp}} \left| \overline{F}_{unp,i} - F_{nom,i} \right|}{n_{unp}}$$

where $\bar{F}_{unp,i}$ is the mean muscle force over all simulations at t_{nom} for the i^{th} unperturbed muscle and n_{unp} the number of unperturbed muscles. This parameter reflects the average effect of the anatomical variability of a specific MT-point on all unperturbed muscle forces in the model.

Secondly, the average difference in calculated muscle force of one specific muscle when perturbing MT-points of all other muscles (OS_{mus}) was calculated for each unperturbed muscle as follows:

$$OS_{mus} = \frac{\sum_{j=1}^{m_{pert}} \left| \overline{F}_{unp,j} - F_{nom} \right|}{m_{pert}}$$

where $\bar{F}_{unp,j}$ is the mean muscle force over all simulations at t_{nom} for the j^{th} perturbed MT-point and m_{pert} the number of perturbed MT-points. This parameter reflects which muscle forces are more sensitive to perturbations of MT-points of other muscles.

Results

The generic model containing the average position, derived from the anatomical variability, for all MT-points is added in Supplementary materials 1.

Anatomical variability of MT-points

Figure 2a and 2b show the absolute and relative variability of individual MT-points (average and standard deviation). The average absolute variability was higher in the AP- (2.15±0.75cm) and ML-dimension (1.89±0.67cm) for the pelvis MT-points, highest in the SI-dimension (2.21±1.01cm) for the femur MT-points, and highest along the AP- and SI-dimension for the tibia MT-points (1.98±0.78cm and 1.49±0.57cm respectively). For all segments, the highest relative variability occurred in the AP-dimension (11.94±4.16%, 21.28±7.09% and 28.18±11.06% for pelvis, femur and tibia, respectively). See supplementary materials 2 for the absolute and relative variability of individual MT-points.

Figures 3 and 4 compare the MT-points in the generic model with the anatomical variability calculated in the MRI-MSMs. Pelvis MT-points not lying within the anatomical variability were more likely to be located too posterior and/or caudal (Fig. 4a). Femur MT-points in the generic model were mainly placed too anterior, whereas the vertical coordinates mainly fall within anatomical variability (Fig. 4b). Tibia MT-point agreement was most variable in the ML-dimension (Fig. 4c).

Local sensitivity

Table 1 lists ΔF and LS_{mtp}. Force of gluteus medius anterior (i, 89N), iliacus (pi, 68N) and adductor brevis (o, 57N) increased most. Force of psoas (pi, -322N and po, -136N) and biceps femoris long head (pi, -105N) decreased most. LS_{mtp} is largest for psoas (pi, 229N and po, 69N) and iliacus (pi, 52N), indicating a more variable response in produced muscle force after perturbation of their MT-point.

Overall sensitivity

Figure 5 shows the average effect of perturbing a specific MT-point on the calculated muscle force of all unperturbed muscles (OS_{mtp}). The perturbed MT-points that induce the largest change in muscle force of the unperturbed muscles belonged to gluteus medius anterior (i, 26±48N), iliacus (pi, 16±35N and po, 11±27N), and psoas (pi, 16±44N and po, 16±38N). See supplementary materials 3 for data of all MT-points.

Figure 6 shows the average difference in calculated muscle force of one specific muscle when perturbing MT-points of other muscles (OS_{mus}). The muscles that were most affected by perturbations in MT-points of other muscles are soleus (47±54N), gastrocnemius medialis (29±32N) and iliacus (24±51N). See supplementary materials 4 for data of all muscles.

The sensitivity of muscle forces (N) in relation to the 3D anatomical variability (in cm³) is shown in figure 7. This figure shows that the muscles with the largest 3D anatomical variability did not show the largest sensitivity of the muscle forces. See supplementary materials 5 for changes in muscle force for all perturbations for all individual MT-points and muscles.

Discussion

Modeling the MT-apparatus for multibody-dynamics simulations of the musculoskeletal system requires assumptions on geometry and dynamics parameters (Erdemir et al., 2007; Pandy and Andriacchi, 2010). Despite the increasing number of sensitivity analyses of model predictions to muscle force generating properties, the influence of the anatomical uncertainty in defining the geometry of MT-models was not extensively investigated. In the present study, we first quantified the

anatomical variability of the MT-point locations by identifying MT-paths based on MR imaging. Then, we adopted a probabilistic method to analyze if muscle forces during gait calculated using a scaled-generic MSM, were affected by the anatomical variability in the MT-paths of hip and knee MT-actuators.

The first objective of this study was to investigate the anatomical variability of MT-points. From the anatomical variability of the MT-points studied, we found the largest relative variability of the MT-points in the AP-dimension (Fig. 2a), while the largest absolute variability of MT-points was observed along the SI-dimension of the femur. Segment-specific anatomical variability patterns were described for the other segments (Fig. 2b). The MT-points with the largest 3D anatomical variability are tensor fasciae latae (via, 39.12cm³), psoas (o, 32.61cm³) and iliacus (o, 22.36cm³) (supplementary materials 2). MT-point selection was deliberately limited to the muscles spanning the hip and knee joints. For the analyzed MT-points, the reported anatomical variability clearly exceeds the errors introduced by the manual segmentation process of the specific workflow. Segmentation errors reported for the intra-rater variability are in the order of 0.18cm, 0.35cm and 0.17cm, for the AP-, SI- and ML-dimensions respectively, and segmentation errors reported for the inter-rater variability are in order of 0.2cm, 0.37cm and 0.15cm, for the AP-, SI- and ML-dimensions respectively (Scheys et al., 2009). The calculated anatomical variability is in line with the results found in Duda et al., 1996, presenting similar attachment areas size on the femur. The origin of vastus lateralis and biceps femoris short head on the femur present less anatomical variability in our study, as MT-points were deliberately placed in the middle of the muscle attachment region for good representation of the MT-path, but therefore inherently limiting the variability of MT-points. Other papers reported anatomical variability of bony structures and landmarks of the lower limb (White et al., 1989; Brand et al., 1982; Kepple et al., 1998; Klein Horsman et al., 2007). However, no direct comparison with the parameters used in the current study is possible. The anatomical variability of the MT-points attaching to the tibia must be interpreted with caution, as not all muscles attaching to the tibia are included. Based on these results, it is concluded that a fixed size perturbation of ±1cm in each dimension, as used in Carbone et al. (2012), is representative of the average anatomical variability of MT-points of the pelvis and femur. However, clear differences between MT-points (supplementary materials 2) are noticed as reflected in the

standard deviation of the average anatomical variability (Fig. 2). A range of 2cm is a large overestimation of the anatomical variability for some MT-points (e.g. the anatomical variability of the Y-dimension of the origin biceps femoris long head is 0.53cm), leading to unrealistically located MT-points. In 3D, a range of 2cm per dimension leads to a 3D anatomical variability of 8cm³. For only a minority of muscle points (n=6) in this study, the reported 3D anatomical variability (ranging between 7cm³ and 9cm³) approximates this value. Therefore, the presented results yield more representative changes is muscle force due to the use of an image-based description of the anatomic variation, based on a small cohort of healthy control subjects (n=12 limbs).

More importantly, several MT-points in the Gait2392 generic model (Delp et al., 2007) do not lie within the reported anatomical variability (Fig. 3 and 4): Only 16 MT-points fall within the reported anatomical variability, whereas 10 MT-points fall outside the anatomical variability. The remainders of the points show variable agreement (supplementary materials 2). Two main reasons can explain these differences. First, the generic model is based on a combination of cadaveric datasets. Our data are extracted from MR-imaging using a standardized workflow. In this workflow, muscles are segmented such that their attachment points are in the middle of the muscle attachment site and their line of action follows the middle of the muscle path. Differences in applied methods to determine the location of the MT-points are most likely to explain the largest part of the disagreement. Second, defining the body reference frames in the subject-specific models is based on the ISB recommendations. Inter-subject variability in bone geometry (Kepple et al., 1998) might influence the orientation of the body reference frame and, thus, influence the relative positioning of MT-points in relation to the bone geometry.

The second objective of this study was to investigate the sensitivity of calculated muscle forces to the reported anatomical variability in MT-geometry. Firstly, ΔF indicates that the muscle, on average, generates a different force when MT-points are perturbed (Table 1). This is due to the different location compared to the generic MT-point location. Secondly, $LSmtp$ (Table 1) indicates the sensitivity of the muscle force to variation of the MT-point location. LS_{mtp} therefore reflects the confidence interval for the calculated muscle forces. These values represent the uncertainty for

specific calculated muscle forces during gait. These should be taken into account when transferring these results to e.g. finite element analysis or the calculation of joint contact forces.

The perturbation of the analyzed MT-points within the anatomical variability also affects the muscle forces of all other muscles in the musculoskeletal model. Firstly, less representative MT-point locations of hip actuators induce most uncertainty in the other muscle forces in the model (Fig. 5). Based on our results, we recommend specific attention when defining the following MT-points: gluteus medius anterior (i), iliacus (po and pi) and psoas (po and pi) (Fig. 5). Secondly, our analysis shows that some calculated muscle forces are more sensitive than others. Soleus, gastrocnemius medialis, tibialis posterior, iliacus, rectus femoris, psoas, tibialis anterior, and gluteus medius are most affected by less representative MT-point positioning of other muscles (Fig. 6). The average effect is not larger than 47N (soleus, Fig. 6). It must, however, be acknowledged that these results are only representative for the MT-points analyzed within this study and cannot be extrapolated for the entire lower extremity, since several lower leg MT-points were not perturbed. MT-location perturbation within the anatomical variability of psoas, iliacus and gluteus medius anterior (i) was mainly compensated by compensatory changes in muscle force of the other two muscles (see supplementary materials 5). In addition, within this study, we have chosen to perturb each MT-point individually. As some muscles share the same attachment sites, simultaneous perturbations of the MT-points could be considered.

This study has some limitations. Firstly, it is important to acknowledge that the scaling of the MT-parameters to account for the change in MT-length following from the perturbation of the muscle points influences the calculated muscle forces and hence the results (Scovil and Ronsky, 2006; Redl et al., 2007; De Groote et al., 2010). We chose linear scaling, which is widely accepted, although other methods have been shown to better preserve the muscle's operating range (Winby et al., 2008). Secondly, calculated sensitivities are dependent on the kinematics. We only calculated the sensitivities for gait kinematics of a young, healthy subject. Hence, the results may not be generalized to other walking speeds, motions or an older/pathological population. Thirdly, the positioning of the subject in the MR-scanner might affect the segmental alignment, which can affect the final musculotendon point location. However, as healthy subjects were recruited, no problems were encountered to position them

in a standardized position in the MR scanner (hip, knee and ankle in neutral position). Therefore, the effect of the subjects' position in the scanner will not substantially affect the anatomical variability of the analyzed musculotendon points. Fourthly, the current workflow only uses one gait stride. However, this approach is similar to the study of Carbone et al. (2012). We did not use different gait patterns, as the inter-subject variability of the gait pattern would add to the variability of muscle forces introduced by perturbing the muscle points. Therefore, such an analysis would not provide a specific answer on the sensitivity of the geometrical perturbations. In this study, we therefore chose a normal kinematics of one control subject. Consequently, the observed differences in muscle force can be solely related to changes in muscle point attachment rather than variability in the gait pattern. However this implies that the current results are representative of healthy subjects with normal bone geometry and a normal gait pattern. Variation in other factors (e.g. gait variability) will only further increase the observed difference in muscle forces. Fifthly, the current study analyzed the change in muscle force for the perturbed simulations (F_{pert}) at the time instant of the maximal muscle force production in the reference simulation (t_{nom}). Post hoc analysis confirmed that this approach has only limited effect on the study outcome as for all perturbed muscles. The time instant of maximal perturbed muscle force was within a range of 2.49 ± 3.57% of t_{nom}. Finally, the reported sensitivity of muscle forces only holds for the current cost function formulation (minimization of muscle activity), which is widely used in simulation using musculoskeletal models.

Interestingly, the muscles with larger anatomical variability do not necessarily present larger sensitivity of the muscle forces, therefore suggesting that the sensitivity of muscle forces and the size of the anatomical variability are not necessarily related and justifying the purpose of this study (Fig. 7). The most sensitive muscles have a rather small 3D anatomical variability (supplementary materials 2).

To our knowledge, this is the first study assessing the sensitivity of muscle forces to the quantified anatomical variability in MT-paths using a probabilistic approach. Therefore, no direct literature comparisons were possible. However, although with different modeling approach the present study led to the similar finding compared to other studies (Carbone et al., 2012; Valente et al., 2014) that calculated MT-forces are most sensitive to the points defining gluteus medius and iliacus paths.

In conclusion, this study quantified the anatomical variability of MT-points in a population of adult control subjects. Several MT-points of the generic model did not fall within this anatomical variability. Furthermore, the local and overall effect of perturbations of MT-point locations within the anatomical variability on muscle force during gait was analyzed. Interestingly, the effect of a perturbation on the muscle force was not directly related to the size of the perturbation, determined based on the observed anatomical variability.

Acknowledgments

This work was funded by KU Leuven's Research Council Grant IDO/07/012 and Research Foundation Flanders (FWO) Grant G.0395.09

Conflict of interest statement

The authors hereby declare there are no financial and personal conflicts of interest.

References

Ackland, D. C., Chung Lin, Y., Pandy, M. G., 2012. Sensitivity of model predictions of muscle function to changes in moment arms and muscle–tendon properties: A Monte-Carlo analysis. Journal of Biomechanics 45, 1463-1471.

Brand, R., Crowninshield, R., Wittstock, C., Pedersen, D., Clark, C., Van Frieken, F., 1982. A model of lower extremity muscular anatomy. Journal of Biomechanical Engineering 104, 304-310.

Carbone, V., van der Krogt, M. M., Koopman, H. F. J. M., Verdonschot, N., 2012. Sensitivity of subject-specific models to errors in musculo-skeletal geometry. Journal of Biomechanics 45, 2476-2480.

De Groote, F., De Laet, T., Jonkers, I., De Schutter, J., 2008. Kalman smoothing improves the estimation of joint kinematics and kinetics in marker-based human gait analysis. Journal of Biomechanics 41, 3390-3398.

De Groote, F., Van Campen, A., Jonkers, I., De Schutter, J., 2010. Sensitivity of dynamic simulations of gait and dynamometer experiments to hill muscle model parameters of knee flexors and extensors. Journal of Biomechanics 43, 1876-1883.

Delp, S. L., Anderson, F. C., Arnold, A. S., Loan, P., Habib, A., John, C. T., 2007. OpenSim: opensource software to create and analyse dynamic simulations of movement. IEEE Transactions of Biomedical Engineering 54, 1940-1948.

Duda, G. N., Brand, D., Freitag, S., Lierse, W., Scheinder, E., 1996. Variability of femoral muscle attachments. Journal of Biomechanics 29, 1185-1190.

Dumas, R., Moissenet, F., Gasparutto, X., Cheze, L., 2012. Influence of joint models on lower-limb musculo-tendon forces and three-dimensional joint reaction forces during gait. Proceedings of the Institution of Mechanical Engineers, Part H: Journal of Engineering in Medicine 226,146-160.

Erdemir, A., McLean, S., Herzog, W., van den Bogert, A.J., 2007. Model-based estimation of muscle forces exerted during movements. Clinical Biomechanics 22, 131-154.

Fregly, B. J., 2009. Design of optimal treatments for neuromusculoskeletal disorders using patient-specific multibody dynamic models. International Journal for Computational Vision and Biomechanics 2, 145-155.

Jansen, K., De Groote, F., Massaad, F., Meyns, P., Duysens, J., Jonkers, I., 2012. Similar muscles contribute to horizontal and vertical acceleration of center of mass in forward and backward walking: implications for neural control. Journal of Neurophysiology 107, 3385-3396.

Kepple, T. M., Sommer, H. J., Lohmann Siegel, K., Stanhope, S. J., 1998. A three-dimensional musculoskeletal database for the lower extremities. Journal of Biomechanics 31, 77-80.

Klein Horsman, M. D., Koopman, H. F. J. M., van der Helm, F. C. T., Prosé, L. P., Veeger, H. E. J., 2007. Morphological muscle and joint parameters for musculoskeletal modelling of the lower extremity. Clinical Biomechanics 22, 239-247.

Lenaerts, G., De Groote, F., Demeulenaere, B., Mulier, M., Van der Perre G., Spaepen, A., Jonkers, I., 2008. Subject-specific hip geometry affects predicted hip joint contact forces during gait. Journal of Biomechanics 41, 1243-1252.

McKay, M. D., Beckman, R. J., Conover, W. J., 1979. A comparison of three methods for selecting values of input variables in the analysis of output from a computer code. Technometrics 21, 239–245.

Pal, S., Langenderfer, J. E., Stowe, J. Q., Laz, P.J., Petrella, A.J., Rullkoetter, P.J., 2007. Probabilistic modeling of knee muscle moment arms: effects of methods, origin-insertion, and kinematic variability. Annals Biomedical Engineering 35,1632-1642.

Pandy, M. G., Adriacchi, T. P., 2010. Muscle and joint function in human locomotion. Annual Review of Biomedical Engineering 12, 401-433.

Redl, C., Gfoehler, M., Pandy, M.G., 2007. Sensitivity of muscle force estimates to variations in muscle-tendon properties. Human Movement Science 26, 306-319.

Scheys, L., Jonkers, I., Loeckx, D., Maes, F., Spaepen, A., Suetens, P., 2006. Image based musculoskeletal modeling allows personalized biomechanical analysis of gait. Lecture Notes in Computer Science 4072, 58-66.

Scheys, L., Loeckx, D., Spaepen, A., Suetens, P., Jonkers, I., 2009. Atlas-based non-rigid image registration to automatically define line-of-action muscle models: A validation study. Journal of Biomechanics 42, 565-572.

Scovil, C. Y., Ronsky, J. L., 2006. Sensitivity of a Hill based muscle-models to perturbations in model parameters. Journal of Biomechanics 39, 2055-2063.

Thelen, D. G., Anderson, F. C., 2006. Using computed muscle control to generate forward dynamic simulations of human walking from experimental data. Journal of Biomechanics 39, 1107-1115.

Valente, G., Taddei, F., Jonkers, I., 2013. Influence of weak hip abductor muscles on joint contact forces during normal walking: probabilistic modeling analysis. Journal of Biomechanics, 46, 2086-2193.

Valente, G., Pitto, L., Testi, D., Seth, A., Delp, S.L., Stagni, R., Viceconti, M., Taddei, F., 2014. Are subject-specific musculoskeletal models robust to the uncertainties in parameter identification? PLoS ONE 9(11): e112625. doi:10.1371/journal.pone.0112625

Viceconti, M., Taddei, F., Cristofolini, L., Martelli, S., Falcinelli, C., Schileo, E., 2012. Are spontaneous fractures possible? An example of clinical application for personalised, multiscale neuro-musculo-skeletal modelling. Journal of Biomechanics 45, 421-426.

White, S., Yack, J., Winter, D., 1989. A three-dimensional musculoskeletal model for gait analysis. Anatomical variability estimates. Journal of Biomechanics 22, 885-893.

Winby, C.R., Lloyd, D.G., Kirk, T.B., 2008. Evaluation of different analytical methods for subject-specific scaling of musculotendon parameters. Journal of Biomechanics 41, 1682-1688.

Wu, G., Siegler, S., Allard, P., Kirtley, C., Leardini, A., Rosenbaum, D., Whittle, M., D'Lima, D. D., Cristofolini, L., Witte, H., Schmid, O., Stokes, I., 2002. ISB recommendation on definitions of joint coordinate system of various joints for the reporting of human joint motion - part 1: ankle, hip and spine. Journal of Biomechanics 35, 543-548.

Xiao, M., Higginson, J., 2010. Sensitivity of estimated muscle force in forward simulation of normal walking. Journal of Applied Biomechanics 26, 142-149.

Zajac, F. E., Neptune, R.R., Kautz, S. A., 2002. Biomechanics and muscle coordination of human walking. Part I: introduction to concepts, power transfer, dynamics and simulations. Gait and Posture 16, 215-32.

Zajac, F.E., Neptune, R.R., Kautz, S. A., 2003. Biomechanics and muscle coordination of human walking: part II: lessons from dynamical simulations and clinical implications. Gait and Posture 17, 1-17.

Figure 1

Outline of the overall workflow: (A) Experimental gait analysis data collection (B) Generation of the nominal dataset using a scaled-generic musculoskeletal model: inverse kinematics (Kalman smoothing), residual reduction algorithm and static optimization are used to obtain a set of muscle forces underlying the measured motion. This set of muscle forces is referred to as the nominal data set (solid line). (C) Documenting anatomical variability based on subject-specific MRI-based musculoskeletal models (MSMs): For each MSM, the 3D location of each musculotendon (MT-) point was expressed in each dimension relative to the dimensions of the bounding box of the segmental bone geometry. Given the six MRI-based MSMs and assuming symmetry between both limbs, 12 relative locations (i.e., the position of the MT-point with respect to the bone dimensions) were defined for each individual MT-point. All together, the minimal and maximal relative values per dimension defined the anatomical variability for that specific MT-point. This dimensional range was then transformed to the corresponding segment of the scaled generic model. (D) Sensitivity analysis: a uniform Latin Hypercube Sampling method generated a library of MT-models containing MT-point locations within the documented anatomical variability. For each MT-model, the static optimization problem was re-solved, resulting in a new set of muscle forces. Muscle forces from the nominal (solid line) and

perturbed data (dotted line) are presented as well as the instant of maximal muscle force in the nominal simulation (t_{nom}, dotted vertical line).

Figure 2

The average (A) absolute (cm) and (B) relative (% of bone dimensions) variability of all MT-points of the pelvis, femur and tibia segment of the unscaled model. The anterior-posterior (light grey), superior-inferior (white) and medio-lateral (dark grey) variability are shown for each segment with standard deviation.

Figure 3a

Anatomical variability (% of bone dimensions) of the pelvic MT-points relative to the generic bone geometry of the pelvis. The anterior-posterior (AP), superior-inferior (SI) and medio-lateral (ML) variability are presented (first, second and third column respectively) with the grey horizontal bar. The black line indicates the unscaled generic MT-point location for the specific dimension. The zero percentage value indicates the posterior, inferior and medial extreme of the segmental bone geometry for the AP-, SI- and ML-dimension respectively. For the ML dimension of the pelvis, the range is from 50 percent (i.e. medial extreme of the right hemi-pelvis) until 100 percent (i.e. lateral extreme of the right hemi-pelvis). For each dimension, an illustrating image of the bone geometry is presented. An axis frame is added to indicate the dimensions along the bone geometry, however note that this is not the body reference frame of the corresponding segment.

Figure 3b

Anatomical variability (% of bone dimensions) of the femoral MT-points relative to the generic bone geometry of the right femur. The anterior-posterior (AP), superior-inferior (SI) and medio-lateral (ML) variability are presented (first, second and third column respectively) with the grey horizontal bar. The black line indicates the unscaled generic MT-point location for the specific dimension. The zero percentage value indicates the posterior, inferior and medial extreme of the segmental bone geometry for the AP-, SI- and ML-dimension respectively. For each dimension, an illustrating image of the bone geometry is presented. An axis frame is added to indicate the dimensions along the bone geometry, however note that this is not the body reference frame of the corresponding segment.

Figure 3c

Anatomical variability (% of bone dimensions) of the tibial MT-points relative to the generic bone geometry of the right tibia. The anterior-posterior (AP), superior-inferior (SI) and medio-lateral (ML) variability are presented (first, second and third column respectively) with the grey horizontal bar. The black line indicates the unscaled generic MT-point location for the specific dimension. The zero percentage value indicates the posterior, inferior and medial extreme of the segmental bone geometry

for the AP-, SI- and ML-dimension respectively. For each dimension, an illustrating image of the bone geometry is presented. An axis frame is added to indicate the dimensions along the bone geometry, however note that this is not the body reference frame of the corresponding segment.

Figure 4

Comparison of the MT-point location of the unscaled generic model to the anatomical variability. Figure 4a, 4b and 4c show the relation of the generic MT-point locations with respect to the anatomical variability for the AP-, SI- and ML-dimension for the pelvis, femur and tibia segment respectively. Generic MT-points can be within the anatomical variability (white bar) or too far posterior/anterior, caudal/cranial and medial/lateral (light grey bar/dark grey bar).

Figure 5

Average difference in calculated muscle force of all unperturbed muscles after perturbation of a specific MT-point (OS_{mtp}). The perturbed MT-points are listed along the horizontal axis and the average difference (± standard deviation) in muscle force (N) of all unperturbed muscles is indicated on the vertical axis. Each MT-point was categorized as origin (o), pseudo origin (po, most distal intermediate point on the proximal segment), pseudo insertion (pi, most proximal intermediate point on the distal segment), insertion (i) or any intermediate via point (via). See supplementary materials 3 for data of all MT-points.

Figure 6

Average difference in calculated muscle force of one specific muscle when perturbing MT-points of other muscles (OS_{mus}). The muscles are listed along the horizontal axis and the average difference (± standard deviation) in muscle force (N) is indicated on the vertical axis. See supplementary materials 4 for data of all muscles.

Figure 7

Relationship between the sensitivity of perturbed muscle forces (LS_{mtp}, see table 1) to the 3D anatomical variability, i.e. the product of the anatomical variability of the three dimensions (cm³) (see supplementary materials 2). The three-dimensional anatomical variability (cm³) and the sensitivity of muscle forces (N) are plotted on the horizontal and vertical axis respectively.

Table 1

Overview of the perturbed MT-points of the scaled generic model and the effect of perturbation within the anatomical variability on the produced muscle force. Each MT-point was categorized as origin (o), pseudo origin (po, most distal intermediate point on the proximal segment), pseudo insertion (pi, most proximal intermediate point on the distal segment), insertion (i) or any intermediate via point (via).

Table 1 documents (i) the MT-point type, (ii) maximal isometric force (F_{max}), (iii) maximal force produced during gait in the nominal simulation (F_{nom}), (iv) average and (v) standard deviation of the perturbed muscle force of 200 simulations ($\bar{F}_{pert}$ and LS_{mtp}) and the (vi) absolute and (vii) relative difference between F_{nom} and $\bar{F}_{pert}$ (ΔF) for every MT-point.

Supplementary materials 1

Unscaled generic model with the averaged MT-point location for 91 documented MT-points.

Supplementary materials 2

Anatomical variability of the documented MT-points. For every MT-point, the following data is presented: (A) the MT-point type (categorized as origin (o), pseudo origin (po, most distal intermediate point on the proximal segment), pseudo insertion (pi, most proximal intermediate point on the distal segment), insertion (i) or any intermediate via point (via)), (B) the corresponding segment, (C) the relative anatomical variability (% of the bone dimensions), (D) the absolute anatomical variability (cm), (E) the absolute three-dimensional anatomical variability (cm³), (F) the minimum location of the MT-point (% of the bone dimensions), (G) the maximum location of the MT-point (% of the bone dimensions), (H) the generic location of the MT-point (% of the bone dimensions) and (I) the agreement of the generic MT-point location with the anatomical variability (yes = within anatomical variability and no = not within anatomical variability). When applicable, dimensional data are indicated with AP (anterior-posterior), SI (superior-inferior) and ML (medio-lateral).

Supplementary materials 3

Average difference in calculated muscle force of all unperturbed muscles when perturbing a specific MT-point (OS_{mtp}). OS_{mtp} ± standard deviation (N) for all perturbed MT-points are listed. Each MT-point was categorized as origin (o), pseudo origin (po, most distal intermediate point on the proximal segment), pseudo insertion (pi, most proximal intermediate point on the distal segment), insertion (i) or any intermediate via point (via).

Supplementary materials 4

Average difference in calculated muscle force of one specific muscle when perturbing MT-points of other muscles (OS_{mus}). OS_{mus} ± standard deviation (N) for all perturbed MT-points are listed.

Supplementary materials 5:

Average absolute difference in muscle force (N) of individual muscles after 200 perturbations of a specific MT-point. The perturbed MT-points are listed horizontally and the individual muscles of the musculoskeletal model are listed vertically.

Table 1

		Muscle forces (in N)				
Muscle	point type	F_{max}	F_{nom}	$\bar{F}_{pert}$	LS_{mtp}	ΔF
Adductor brevis	o	429	59	117	4	57
	i	429	59	5	7	-54
Adductor longus	o	627	175	206	2	31
	i	627	175	142	12	-33
Adductor magnus posterior	o	488	80	106	6	26
	i	488	80	89	1	9
Biceps femoris long head	o	896	156	138	19	-18
	pi	896	156	51	25	-105
Biceps femoris short head	o	804	176	204	1	29
	pi	804	176	77	34	-99
Gastrocnemius lateralis	po	683	150	138	6	-12
Gastrocnemius medialis	po	1558	579	541	10	-38
Gluteus maximus anterior	po	573	97	118	4	21
	pi	573	97	81	11	-15
Gluteus maximus middle	po	819	178	189	9	11
	pi	819	178	170	13	-7
Gluteus maximus posterior	po	552	79	102	5	24
	pi	552	79	81	9	2
Gluteus medius anterior	o	819	449	408	28	-42
	i	819	449	538	17	89
Gluteus medius middle	o	573	173	167	3	-6
	i	573	173	184	8	12
Gluteus medius posterior	o	653	187	186	2	-1
	i	653	187	172	10	-15
Gluteus minimus anterior	o	270	88	109	12	21
	i	270	88	87	4	-1
Gluteus minimus middle	o	285	49	47	7	-2
	i	285	49	43	3	-6
Gluteus minimus posterior	o	323	46	43	1	-3
	i	323	46	34	5	-12
Iliacus	po	1073	659	651	20	-8
	pi	1073	659	728	52	68
Piriformis	po	444	91	133	7	42
	i	444	91	66	21	-25
Psoas	po	1113	538	402	69	-136
	pi	1113	538	216	229	-322
Quadratus femoris	o	381	101	109	2	8
	i	381	101	96	4	-5
Rectus femoris	o	1169	299	309	8	10
Sartorius	o	156	21	23	1	3
	via	156	21	22	0	1
Semimembranosus	o	1288	359	366	39	7
	pi	1288	359	353	27	-6
Semitendinosus	o	410	48	44	1	-3
	pi	410	48	38	1	-9
Tensor fasciae latae	o	233	65	77	6	12
	via	233	65	65	4	0
	via	233	65	63	0	-2
	i	233	65	63	0	-2
Vastus intermedius	po	1365	138	131	0	-7
Vastus lateralis	po	1871	258	255	3	-4

Figure 1

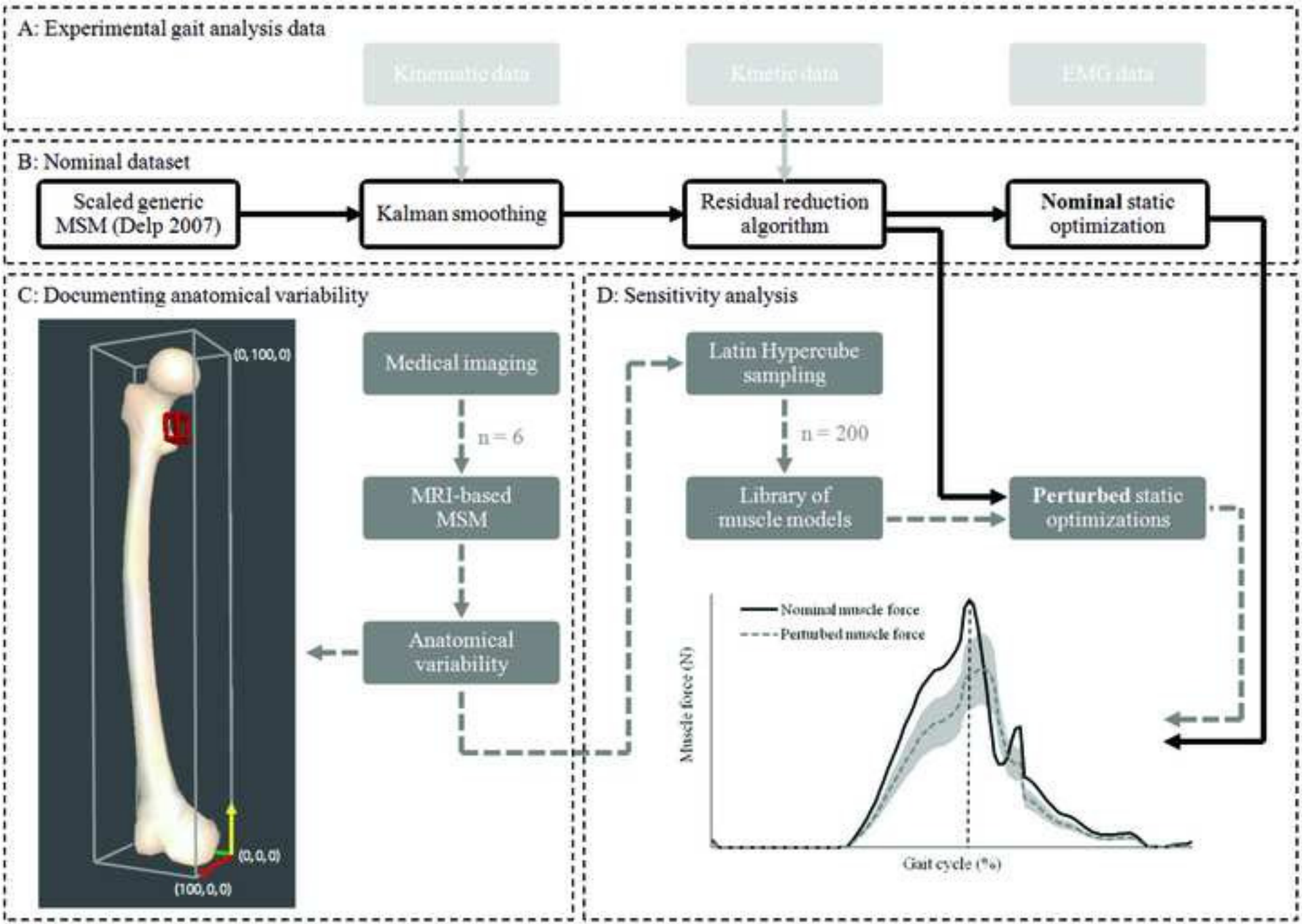

Figure 2

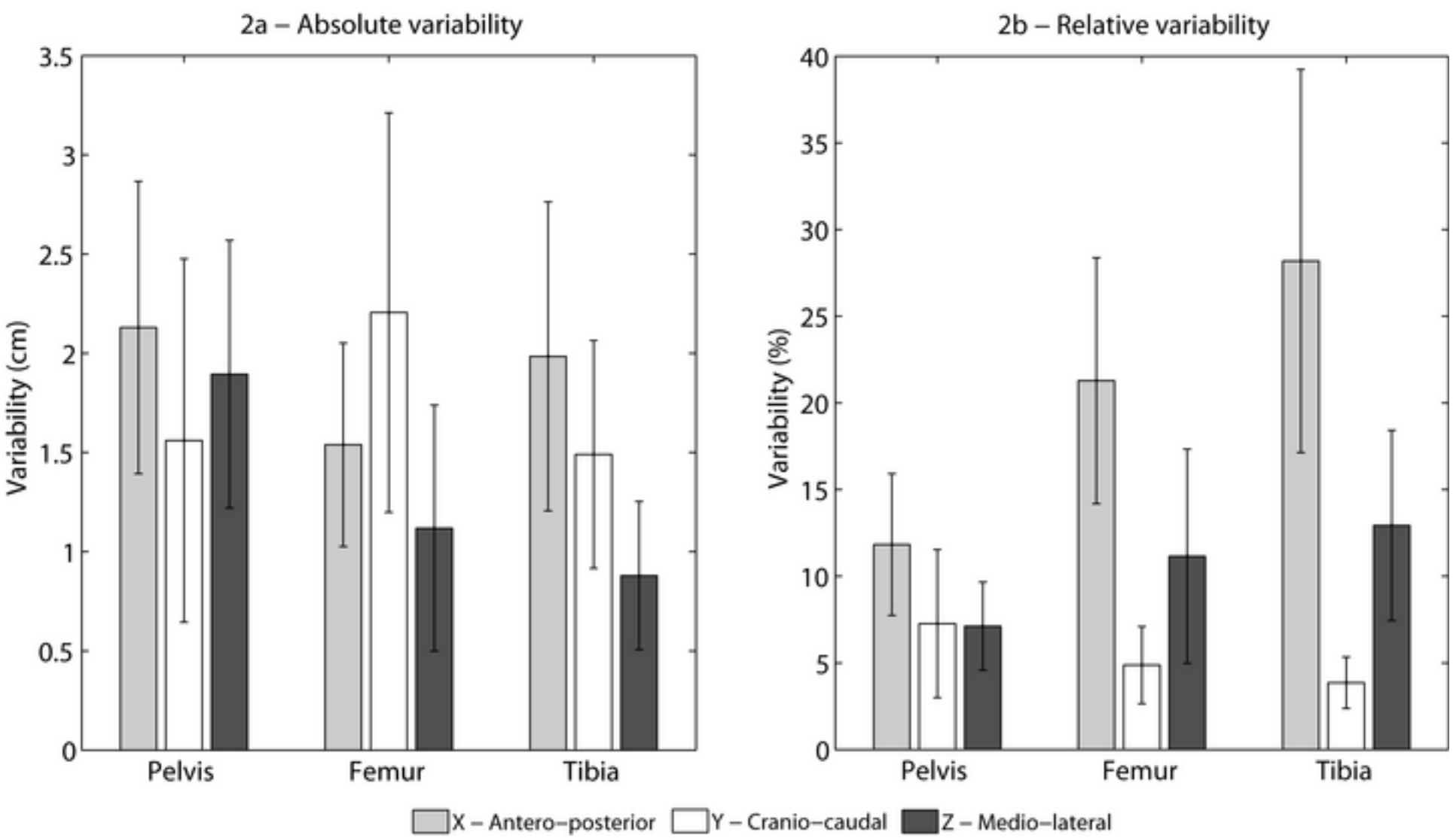

Figure 3a

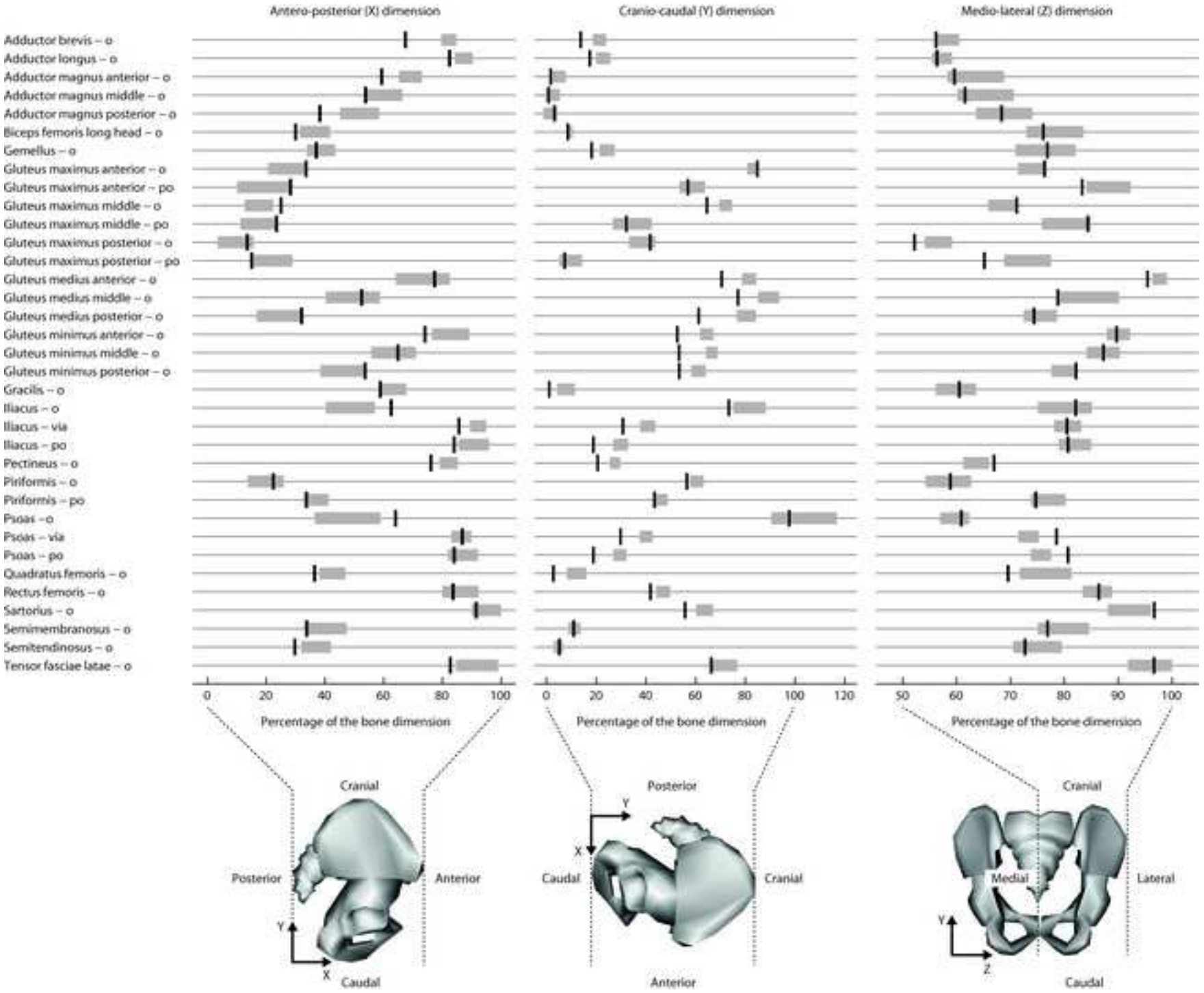

Figure 3b

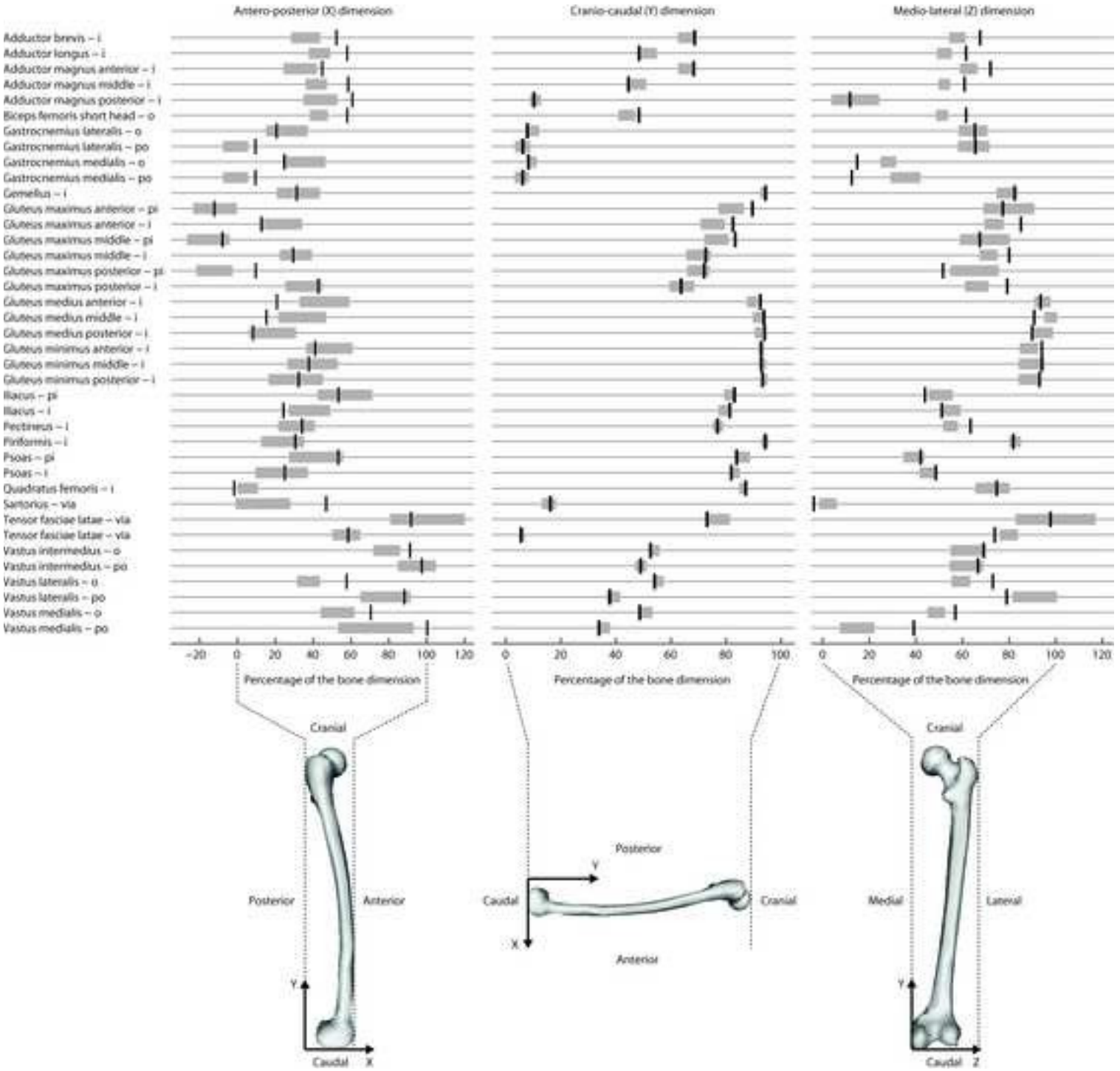

Figure 3c

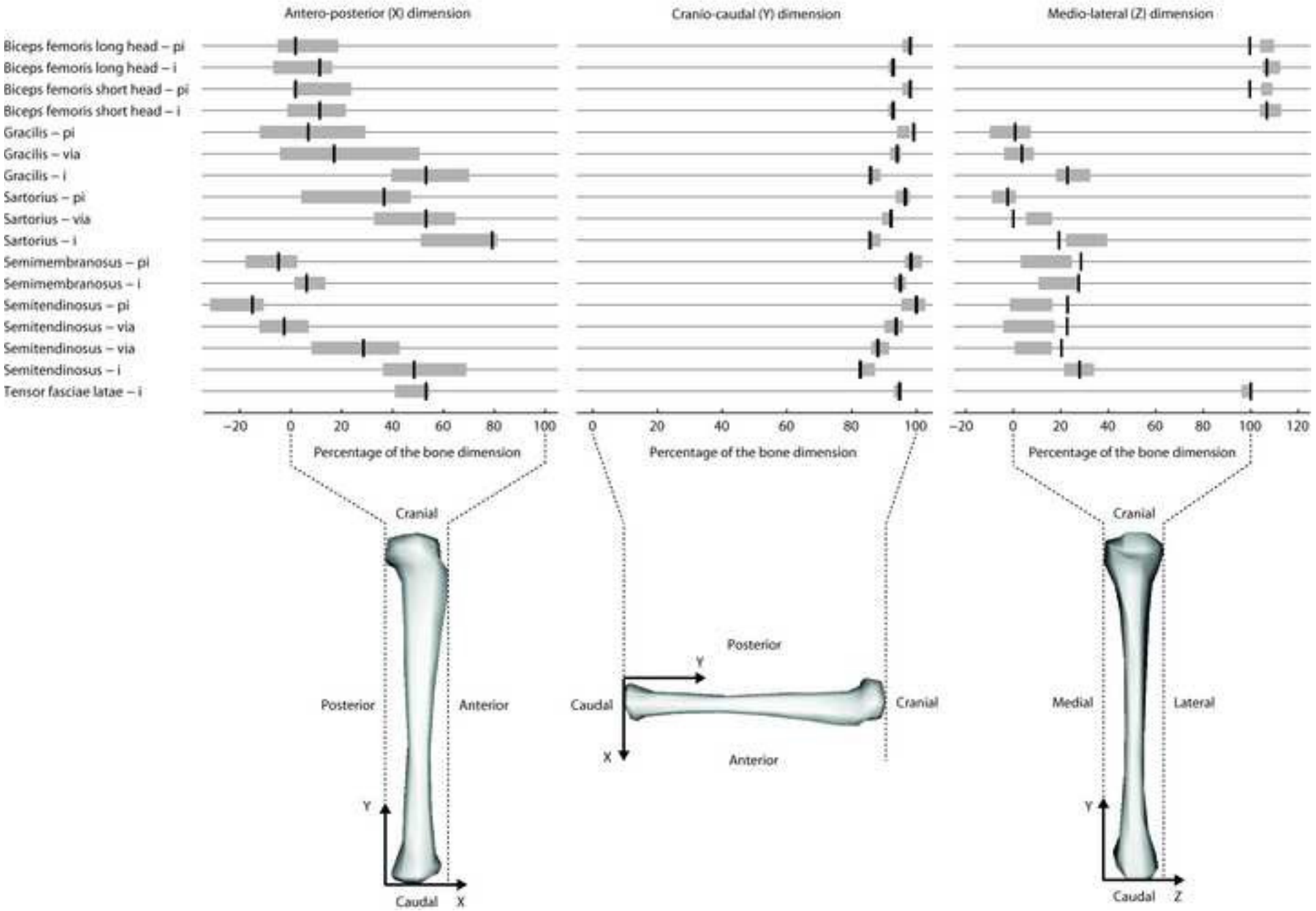

Figure 4

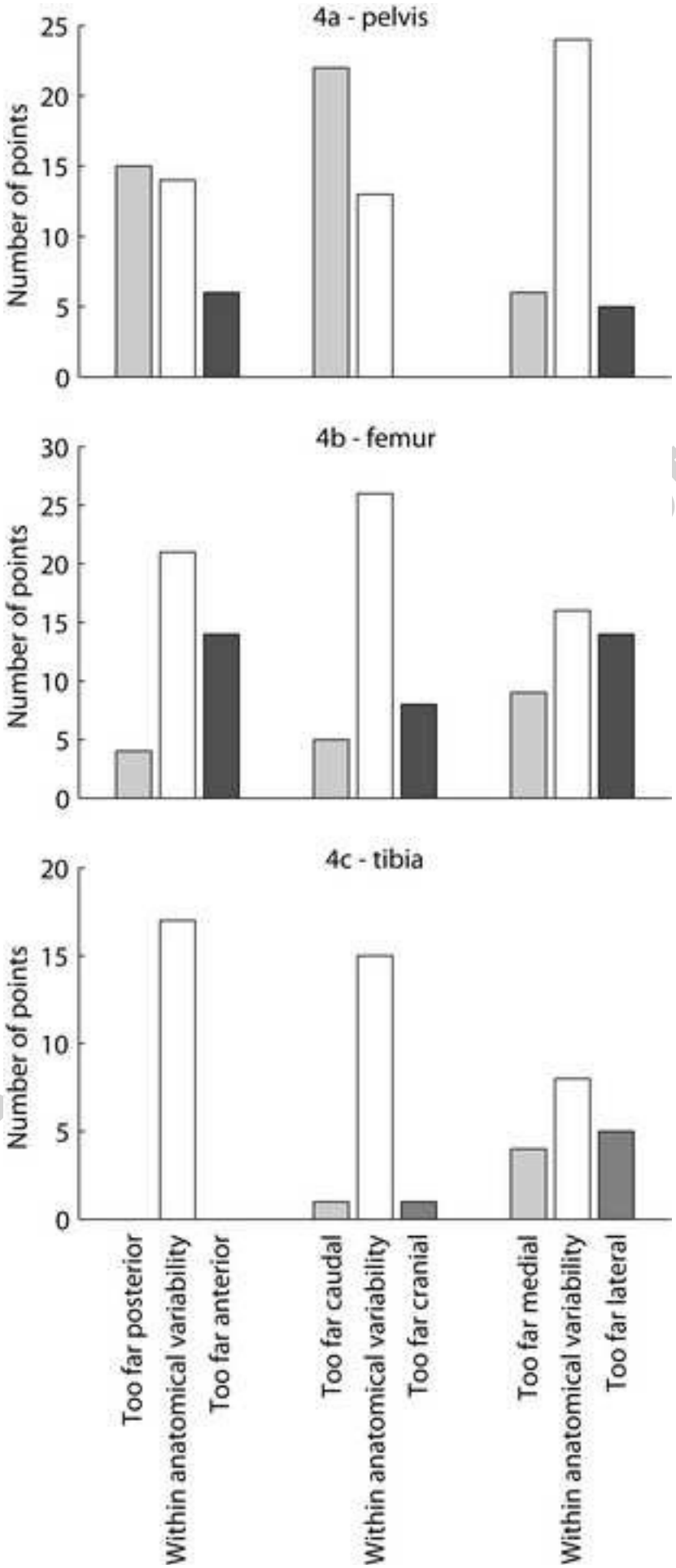

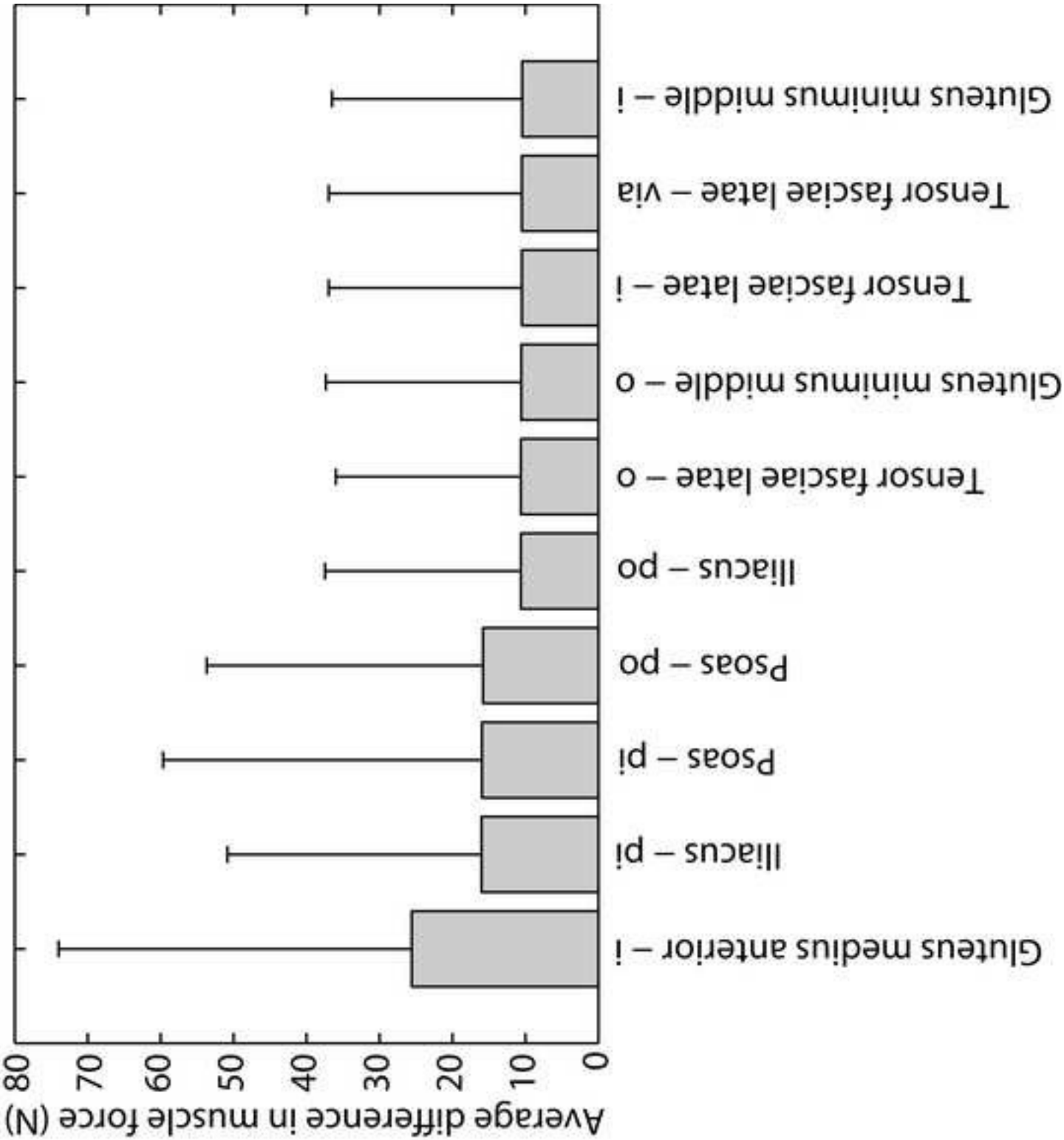
Average difference in muscle force (N)
0
10
20
30
40
50
60
70
80
Gluteus medius anterior – i
Iliacus – pi
Psoas – pi
Psoas – po
Iliacus – po
Tensor fasciae latae – o
Gluteus minimus middle – o
Tensor fasciae latae – i
Tensor fasciae latae – via
Gluteus minimus middle – i

Figure 5

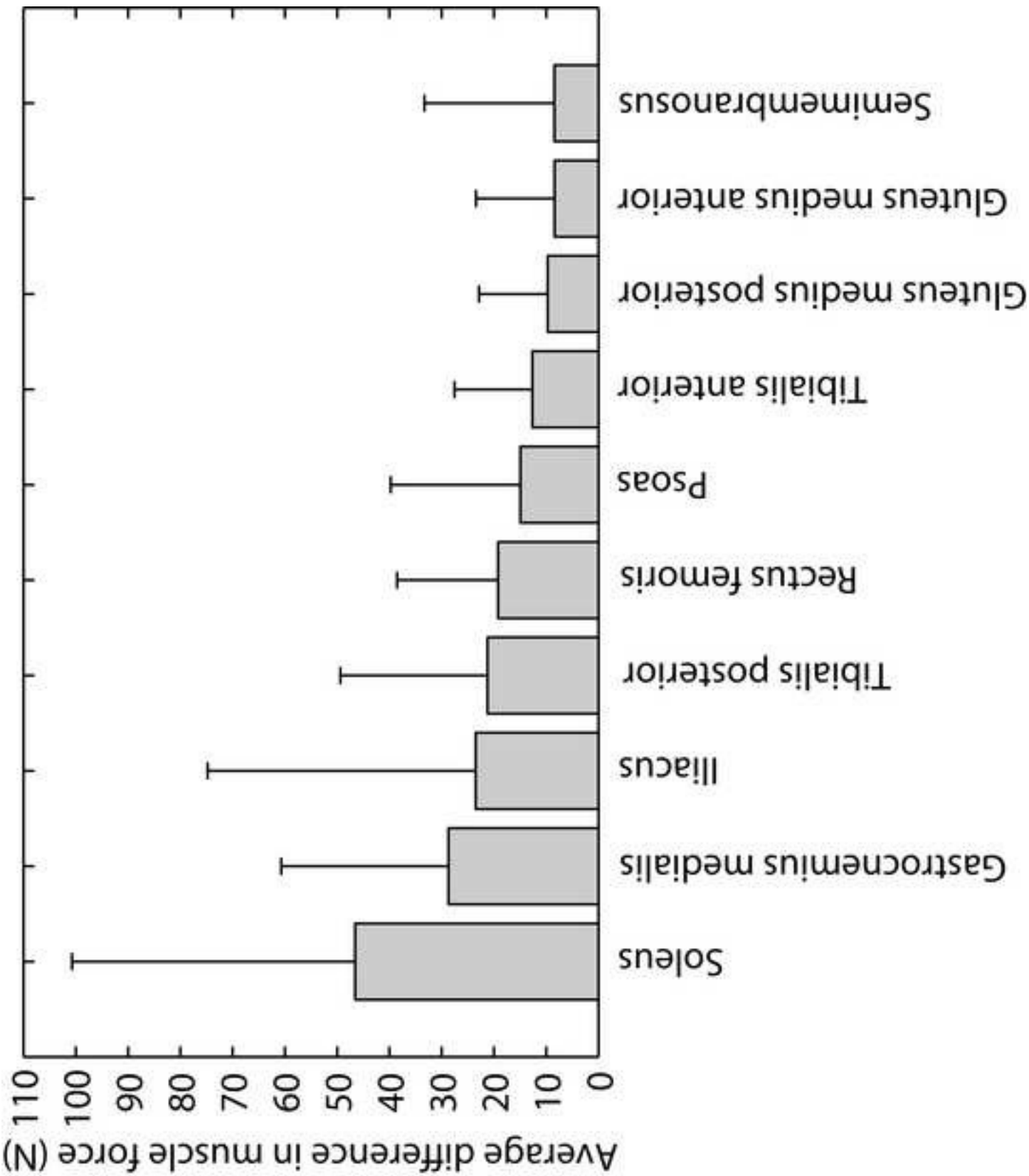
Average difference in muscle force (N)
0
10
20
30
40
50
60
70
80
90
100
110
Soleus
Gastrocnemius medialis
Iliacus
Tibialis posterior
Rectus femoris
Psoas
Tibialis anterior
Gluteus medius posterior
Gluteus medius anterior
Semimembranosus

Figure 6

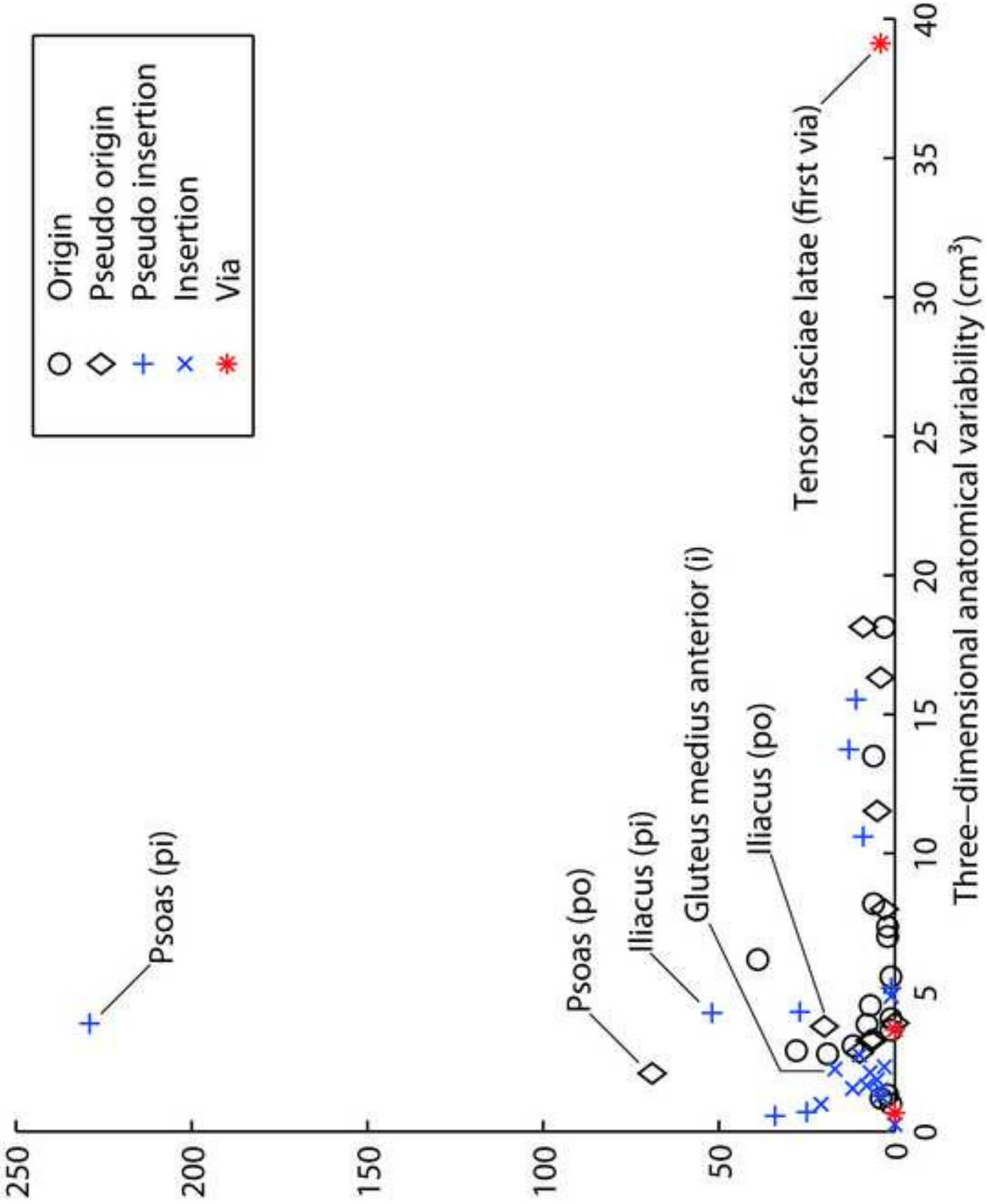
Origin
Pseudo origin
Pseudo insertion
Insertion
Via
Psoas (pi)
Psoas (po)
Iliacus (pi)
Gluteus medius anterior (i)
Iliacus (po)
Tensor fasciae latae (first via)
Sensitivity of muscle force (N)
Three−dimensional anatomical variability (cm³)
250
200
150
100
50
0
0
5
10
15
20
25
30
35
40

Figure 7